TDDFT Study of One- and Two-Photon Absorption Properties: Donor−π−Acceptor Chromophores

Paul N. Day,* Kiet A. Nguyen, and Ruth Pachter

Materials and Manufacturing Directorate, Air Force Research Laboratory, Wright Patterson Air Force Base, Ohio 45433

Received: June 9, 2004; In Final Form: September 27, 2004

We report a comprehensive time-dependent density functional theory (TDDFT) study of one-photon and two-photon absorption (OPA and TPA, respectively) spectra for donor−π−acceptor molecules. The calculated excitation energies were generally shown to be in good agreement with experiment, particularly when compared to results from measurements carried out in a nonpolar solvent, although the oscillator strengths were overestimated in some cases. Calculated TPA cross sections applying the two-state approximation were shown to be highly dependent on the form of the line-shape function used. Although a good agreement with experimental TPA spectra was generally observed, the wide range in the experimentally measured values and lack of systematic experimental data on solvent effects limited a detailed comparison as yet.

1. Introduction

Compounds that exhibit large TPA cross sections have a variety of potential applications such as 3D optical storage memory,[1] confocal microscopy,[2] upconversion lasing, and photodynamic therapy.[3] Of particular interest are so-called donor−π−acceptor (D−π−A) compounds, where electron donating and accepting groups are attached to a core having a delocalized π-electron structure, such as stilbene or fluorene. Substituted stilbenes have been of interest for some time as two-photon absorption (TPA) materials,[4−14] and diphenylamino-fluorene-based chromophores have more recently also been recognized for having large TPA cross sections. Thus, there has been considerable interest[15−17] in applying theoretical methods to establish structure-to-property relationships and provide strategies for the design of such chromophores.

Time-dependent density functional theory (TDDFT) has been shown to consistently give accurate excitation energies and oscillator strengths, especially for low-lying states,[18−20] and particularly when employing hybrid exchange-correlation functionals. In this study, we compared the results from two different hybrid functionals, namely, PBE0 and B3LYP, while noting that, in a previous study, several other common hybrid functionals were tested and found to yield similar excitation energies and oscillator strengths.[21] The second-order or quadratic response within the TDDFT formulation can be used to calculate the TPA cross section,[22] either by obtaining the analytical TPA probability from the residue of the quadratic response or by calculation of the excited-state-to-excited-state transition dipole moments, which are needed to compute the TPA rate by the sum-over-states (SOS) method. The former has been applied by Salek et al.[23] to several small molecules, while transition dipole moments between excited states were recently calculated for modeling three-photon absorption.[24] An approximation to quadratic TDDFT was also implemented[25] for the calculation of excited-state-to-excited-state transition dipole moments, but the accuracy of this method has not been confirmed.[21] Most recently, TDDFT has been applied for calculating TPA parameters for a series of centrosymmetric chromophores based on [2.2]-paracyclophane.[26] In this study, we aim to assess the validity of calculating TPA cross sections using the two-state approximation for non-centrosymmetric molecular systems, which does not require the excited-state-to-excited-state transition dipole moments and which has been shown to provide a good approximation to the TPA cross section using the random phase approximation (RPA).

Although a number of previous theoretical studies at various levels of theory, primarily semiempirical, have reported TPA cross section predictions for substituted stilbenes or fluorenes,[10,27−29] our goal was to carry out a systematic comparison between the theoretical results and experimental values obtained from femtosecond (fs) experiments, minimizing the effects of other processes. In this investigation, we therefore first examined the excitation energies and transition dipole moments for a series of donor−acceptor substituted stilbene-based compounds in order to predict both the linear absorption and the two-photon absorption spectra. Our choice of molecules resulted from the available experimental fs cross section data for D−π−A molecules, consisting of a central π-conjugated moiety, either stilbene (denoted CC), azobenzene (denoted NN), or a hybrid of these two molecules (denoted CN or NC), following the notation in the work by Antonov et al.,[12] for which TPA cross sections using the *Z*-scan technique[30] with 130 fs laser pulses were reported. Each molecule has an electron donor group on one end and an electron acceptor on the other end; electron acceptor groups include nitro (denoted A) and the weaker acceptor cyano (denoted a), while electron donors include dimethyl amino (denoted D) and the weaker donor amino (denoted d). Thus, 4-dimethylamino-4′-nitrostilbene (DANS) is denoted ACCD and 4-dimethylamino-4′-nitroazobenzene is denoted ANND. In addition to these two compounds, ANCD, ACND, ANNd, and aNND were also studied, and the results were compared to experiment. All molecular structures are shown in Figure 1. To further assess the applicability and range of accuracy that can be achieved with the two-level approximation within linear response TDDFT, we also selected available fs TPA spectra for fluorene and fluorene-based donor−acceptor AFX chromophores (X is a number unique to each chro-

* Corresponding author.

10.1021/jp047511i CCC: $30.25
Published on Web 01/19/2005

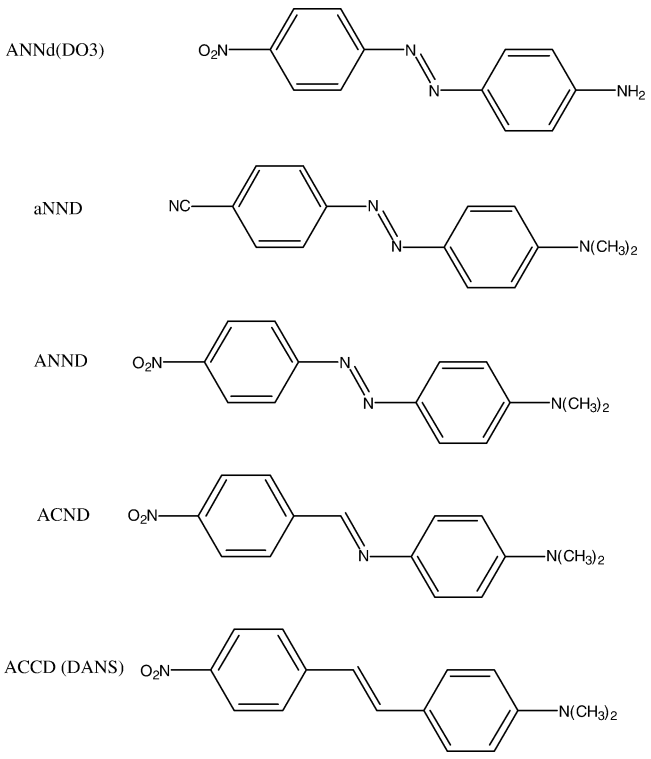

Figure 1. Structures of the stilbene-based compounds.

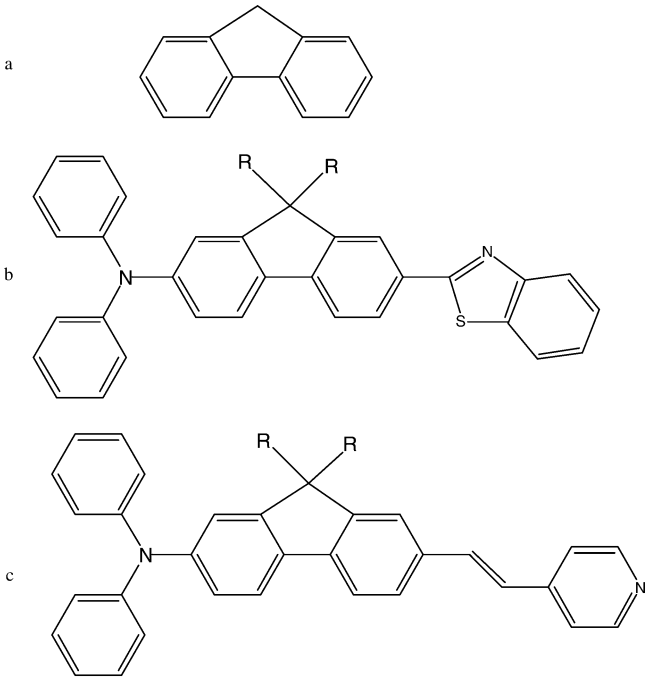

Figure 2. Structures of (a) fluorene, (b) AF240 (R = ethyl) and AF69 (R = decyl), and (c) AF50 (R = decyl) and AF50P [R = ethyl, N = C−PO(OCH_2H_5)$_2$].

mophore; structures shown in Figure 2.) Symmetry-adapted-cluster configuration interaction (SAC-CI) calculations for fluorene were also carried out for further validation.

In all materials studied, excited states are both one- and two-photon "allowed", and therefore, we examined the one-photon absorption (OPA) properties. Overall, our calculations offer a preliminary assessment of the application of TDDFT in the linear response regime, to then enable applications for large systems that exhibit increased TPA, as recently shown, for example, for a conjugated porphyrin dimer,[31] and provide the basis for future studies theoretically, also including vibronic[32,33] and solvent effects.[34]

2. Theoretical Methods

2.A. Electronic Structure. The structures were predicted using the Kohn−Sham (KS)[35] density functional theory with the 6-311G(d,p)[36,37] basis set for the stilbene-based compounds and with the 6-31G(d)[38,39] basis set for the fluorene-based compounds, since the basis set effects were found to be rather small for the latter. DFT calculations were carried out using Becke's three-parameter hybrid exchange-correlation (x-c) functional,[40−44] hereafter referred to as B3LYP. The optimized geometries were all confirmed as minima by Hessian calculations. While the stilbene-based molecules are close to having C_s symmetry, all the minima are C_1. The largest deviation from C_s symmetry for stilbene-based systems is due to the tendency of the amino group to be pyramidal. In contrast, the three α-carbons and amino nitrogen are essentially coplanar in the fluorene-based systems. The coordinates of all the optimized geometries are available in the Supporting Information.

Excitation energy calculations were carried out using TDDFT,[45−47] as implemented in the Gaussian 98[48] and Gaussian 03[49] programs. TDDFT calculations, carried out at the B3LYP structures, were done using the same basis sets as those used in the ground-state DFT calculations (except for fluorene where noted). Both B3LYP and the hybrid functional of Perdew, Burke, and Erzerhof, known as PBE0[50,51] (PBE1PBE in Gaussian), were used for the TDDFT. In PBE0, the fraction of exact exchange is set to 0.25 on theoretical grounds, while, in B3LYP, it was empirically optimized to 0.20. The ground- and excited-state dipoles were computed using the one-sided finite field method with an applied field of 10^{-4} au, which was found to give more accurate results than 10^{-3} au, which was suggested in the program user manual. Slight changes in dipole moments are noted when computed using central difference. Variational SAC-CI calculations with singles and doubles linked excitations (SD-R)[52−55] were carried out using the SAC-CI program included in the Gaussian 03 suite of programs.

2.B. One-Photon Absorption. The one-photon absorption (OPA) oscillator strength of an electronic transition from the ground state (0) to the final state (f) can be obtained by

$$f_{0f} = \frac{8\pi^2}{3}\frac{m_e}{e^2 h}\nu_{0f}|\mu_{0f}|^2 \tag{1}$$

where m_e is the electron mass, e is the electron charge, h is Planck's constant, $\nu_{0f} = E_{0f}/h$ is the frequency in s^{-1} corresponding to the transition energy (E_{0f}) between the two states, and the transition dipole moments are given by

$$\mu_{0f} = \langle 0|e\mathbf{r}|f\rangle \tag{2}$$

The computed oscillator strength is related to the experimental integrated intensity by

$$f_{0f} = 4.32 \times 10^{-9}\int \epsilon(\bar{\nu})\, d\bar{\nu} \tag{3}$$

where ϵ is the extinction coefficient in units of L mol^{-1} and $\bar{\nu}$ is the frequency in cm^{-1}. Since the integration limits in eq 3 are generally not known, a single Gaussian (or Lorentzian) function is often used to represent an experimental spectral band, which gives rise to an approximate measure of the corresponding band intensity. Using a Gaussian line-shape,

$$f_{0f} = 4.32 \times 10^{-9} \epsilon_{max} \int e^{-(\Delta\bar{\nu}/\theta)^2} \, d\bar{\nu} = 4.32 \times 10^{-9} \sqrt{\pi} \epsilon_{max} \theta \quad (4)$$

The θ width parameter relates to the full width (W) at half-maximum ($\epsilon_{max}/2$) by $W = 2(\ln 2)^{1/2}\theta$, and the cross section (in square centimeters) at the band maximum relates to ϵ_{max} by $\sigma_{max} = 3.83 \times 10^{-21} \epsilon_{max}$. Thus, ϵ_{max} or σ_{max} of a transition can be readily approximated, provided its bandwidth is known.

2.C. Two-Photon Absorption. The TPA cross section can be obtained by relating the absorption rate to the TPA transition probability, which was first derived by Goppert-Mayer using second-order perturbation theory.[56] The exact form of the TPA cross section [$\delta_{f0}(E_1 + E_2)$] depends on the rate expression, and in order to be consistent with the experimental studies, we define it as outlined in the following. The TPA rate from a single beam is given by[57]

$$\frac{dI_1}{dz} = -\frac{\delta_{f0}(2E_1)N}{E_1} {I_1}^2 \quad (5)$$

and from two distinguishable beams, the TPA rate is

$$\frac{dI_1}{dz} = -2N\frac{\delta_{f0}(E_1 + E_2)}{E_2} I_1 I_2 - \frac{\delta_{f0}(2E_1)N}{E_1} {I_1}^2 \quad (6a)$$

$$\frac{dI_2}{dz} = -2N\frac{\delta_{f0}(E_1 + E_2)}{E_1} I_1 I_2 - \frac{\delta_{f0}(2E_2)N}{E_2} {I_2}^2 \quad (6b)$$

where $E_1 = h\nu_1$ and $E_2 = h\nu_2$ are the photon energies, h is Planck's constant, ν (s^{-1}) is the frequency of the light, I (erg cm^{-2} s^{-1}) is the light intensity for each beam, z (cm) is the direction of light propagation, and N (molecules cm^{-3}) is the molecular density of the absorbing material. Using these definitions, the TPA cross section (δ_{f0}) (cm^4 s photon^{-1} molecule^{-1}) is the same for both single-beam and two-beam processes and is written as[14,57,58]

$$\delta_{f0}(E_1 + E_2) = \frac{8\pi^4}{(ch)^2} E_1 E_2 g(E_1 + E_2) |S_{f0}|^2 \quad (7)$$

where c is the speed of light, S_{f0} is the two-photon matrix element for a two-photon transition between the ground state and the final state (f), and $g(E_1 + E_2)$ is the normalized line-shape function. In eq 6b, if $I_2 \ll I_1$, such as in a pump−probe experiment, the second term is negligible. If E_1 is much less than half of the transition energy, the second term in eq 6a is also negligible and all TPA will be the result of the "cross-term", which represents the process whereby one photon is absorbed from each beam. In some formulations, the TPA rate was defined as half of the expression in eq 6, and thus, the corresponding value for the TPA cross section was twice that given in eq 7.[17,59,60] The line-shape can be represented by a Gaussian function

$$g^G(E_1 + E_2) = \left(\frac{4h^2 \ln 2}{\pi {E_{fwhm}}^2}\right)^{1/2} \exp\left[\frac{-4 \ln 2}{{E_{fwhm}}^2}(E_1 + E_2 - E_f)^2\right] \quad (8)$$

or by a Lorentzian

$$g^L(E_1 + E_2) = \frac{h}{\pi} \frac{E_{fwhm}/2}{(E_1 + E_2 - E_f)^2 + (E_{fwhm}/2)^2} \quad (9)$$

where E_{fwhm} is the full width at half-maximum for the final state (f) and E_f is the energy of state f relative to the ground state. Previously computed TPA cross sections used either Gaussian[61−63] or Lorentzian[14,17] line-shapes. Note that, when a Gaussian function is used, the calculated peak TPA cross section is 1.48 times larger than that for a Lorentzian, for a given line width.

In this study, both photons are assumed to have the same energy (E_λ). In this case, the orientationally averaged expression for the two-photon matrix elements for linearly polarized photons with parallel polarization is given by[60,64,65]

$$|S_{f0}|^2 = \frac{4}{15}\sum_j^N \sum_k^N \left\{ \begin{array}{l} \dfrac{(\langle k|\mu|0\rangle \cdot \langle f|\mu|k\rangle)\langle j|\mu|0\rangle(\cdot\langle f|\mu|j\rangle)}{[(E_k - E_\lambda)(E_j - E_\lambda) + \Gamma^2]} \\ + \dfrac{(\langle k|\mu|0\rangle \cdot \langle j|\mu|0\rangle)(\langle f|\mu|k\rangle \cdot \langle f|\mu|j\rangle)}{[(E_k - E_\lambda)(E_j - E_\lambda) + \Gamma^2]} \\ + \dfrac{(\langle k|\mu|0\rangle \cdot \langle f|\mu|j\rangle)(\langle f|\mu|k\rangle \cdot \langle j|\mu|0\rangle)}{[(E_k - E_\lambda)(E_j - E_\lambda) + \Gamma^2]} \end{array} \right\} \quad (10)$$

where the sums over j and k include the ground state and all excited states. The damping factor for one-photon transitions (Γ) has been set to 0.05 eV in all calculations to prevent the TPA cross section from "blowing up" near a one-photon resonance. The photon energies reported are well below the first one-photon resonance, so Γ is insignificant.

Two types of processes characterize two-photon absorption. Type I TPA is mediated by one or more "intermediate" states, each of which must have significant transition dipoles with both the final state ($\mu_{fj} = \langle f|e\mathbf{r}|j\rangle$) and the ground state ($\mu_{0j} = \langle 0|e\mathbf{r}|j\rangle$) and also have a transition energy reasonably close to the photon energy, if it is to make a significant contribution to the TPA cross section. Often, the sums in eq 10 can be approximated by including just one such intermediate state.[4,61,66,67] When the single intermediate approximation, known as the "three-state" model, is used in eqs 7−10 and both photons are assumed to have the same energy (E_λ), the expression for the maximum TPA cross section for type I TPA becomes

$$\delta_{f0}^I = \frac{32\pi^4 g_{max}}{15(ch)^2} \frac{{E_\lambda}^2}{(E_j - E_\lambda)^2} |\mu_{0j}|^2 |\mu_{jf}|^2 (2\cos^2 \Theta_{\mu\mu} + 1) \quad (11)$$

where $\Theta_{\mu\mu}$ is the angle between the two transition dipole moments (μ_{0j} and μ_{jf}) and g_{max} is the maximum value of the line-shape function, which can be obtained from eq 8 or 9 by setting $E_f = E_1 + E_2 = 2E_\lambda$. This maximum is inversely proportional to the line width; thus, the value used for the line width has a large effect on the computed peak TPA cross section.

In type II TPA, a strongly allowed one-photon state can be TPA allowed provided there is a change in dipole moment between the ground state and the final state ($\Delta\mu_{0f}$). In this case, the first excited state may dominate the TPA, and the sum can be carried out with just the ground state and the first excited state. The maximum TPA cross section for type II TPA in this two-state approximation is given by[17,61]

$$\delta_{f0}^{II} = \frac{32\pi^4 g_{max}}{15(ch)^2} |\mu_{0f}|^2 |\Delta\mu_{0f}|^2 (2\cos^2 \Theta_{\mu\Delta\mu} + 1) \quad (12)$$

where now $\Theta_{\mu\Delta\mu}$ is the angle between the transition dipole moment and the dipole difference vector.

TABLE 1: Excitation Energies (eV), Dipole Moments (D), and Transition Moments (D) for ACCD, Including Measured Values in Ten Different Solvents and Seeded in a Supersonic Expansion (SSE)[a]

	E_{0f} (eV)	μ_{00} (D)	μ_{0f} (D)	μ_{ff} (D)	$\Delta\mu_{0f}$ (D)
CNDO/S[5]	3.49	10.4	7.0	36.5	26.1
AM1, SCI = 4[6]	3.13	9.3		18.8	9.5
CNDOVS[6]	2.83	9.1		17.7	8.7
INDO/MRD-CI[7]	3.68	10.3	8.6	21.7	11.4
PPP[8]	3.29				
AM1 CI[9]	3.01	8.1	7.6	12.4	4.3
ab initio 6-31G[10]	3.37	9.0	9.0	19.4	10.4
PM3, CI = 20[11]	3.62	8.0	8.1	17.1	9.1
AM1, CI = 15[11]	3.68	9.0	8.3	18.6	9.6
SAM1, CI = 16[11]	3.67	8.6	8.9	21.7	13.1
this work (B3LYP)	2.73	10.7	8.8	26.1	15.4
this work (PBE0)	2.88	10.6	9.1	25.7	15.1
measured in SSE[70]	3.69				
gas-phase fit 1[b]	3.35				
gas-phase fit 2[c]	2.94				
measured in cyclohexane[8]	2.98				
measured in cyclohexane[77]	3.08		7.1		
measured in cyclohexane[11,80]		8.2		19.2	11.0
measured in benzene[77,92]	2.87				
measured in benzene[81,93]	2.85	7.1		26.0	18.9
measured in dibutyl ether[8]	2.96				
measured in diethyl ether[8]	2.95				
measured in ethyl acetate[8]	2.91				
measured in THF[8]	2.86				
measured in acetonitrile[8]	2.89				
measured in ethanol[92]	2.88				
measured in chloroform[8]	2.84		6.9		
measured in chloroform[82]	2.83	6.7	8.2		
measured in chloroform[94]	2.88	6.6			
measured in DMSO[12]	2.74		7.4		

[a] The final state (*f*) refers to the first excited state, which is used in the two-state approximation given by eq 12. [b] McRae−Bayliss[71−74] model fit to the measured data and extrapolated to the gas phase.[70] [c] Onsager[75,76] model fit to the measured data and extrapolated to the gas phase.[70]

Centrosymmetric chromophores, such as all-trans octatetraene, stilbene, or symmetrically substituted stilbene-based[14] molecules, exhibit TPA by the type I mechanism, while non-centrosymmetric molecules, such as the donor−acceptor substituted stilbene-based compounds examined in this study as well as the AFX chromphores,[68,69] undergo TPA primarily by the type II mechanism. All the molecules we investigated undergo type II TPA, and the two-state approximation was used to calculate the TPA cross sections.

3. Results and Discussion

3.A. Stilbene-Based Donor−Acceptor Molecules. Previous theoretical results, experimental data, and our calculated TDDFT values with the B3LYP and PBE0 x-c functionals are summarized in Table 1 for ACCD. In comparing our results to experiment, it is first important to consider the effects of the medium. The experimental studies of OPA include measurements in several solvents and also seeded in a supersonic expansion (SSE).[70] In the same study,[70] measured excitation energies in solution were fitted to the McRae−Bayliss[71−74] and Onsager[75,76] models and extrapolated to the gas phase, as reported in Table 1. The Onsager model yields a gas-phase excitation energy similar to that measured in the nonpolar solvent cyclohexane,[8,77] while the McRae−Bayliss model gives an excitation energy midway between that from the Onsager model and that measured in the SSE; the large difference in the three gas-phase excitation energies is still unclear. It is notable that the TDDFT excitation energy using the PBE0 (x-c) functional is in good agreement with the OPA measured value in a nonpolar solvent, and it also agrees with the Onsager model. The B3LYP excitation energy for ACCD (2.73 eV) is in only fair agreement with the measured results carried out in nonpolar solvents, rendering this (x-c) functional less accurate than PBE0. This could be partially due to the tendency of B3LYP to slightly underestimate excitation energies for this class of compounds. Interestingly, most of the calculated excitation energies reported previously (Table 1) are not consistent with the experimental results in the most nonpolar solvents (cyclohexane and benzene), where the solvent is unlikely to have a significant effect on the excitation energy. Overall, our good agreement with the spectra measured in cyclohexane and benzene is encouraging, as the excitation energy ranges from 2.98 to 3.08 eV. It is noted that excitation energies of 2.88 and 2.89 eV were measured in ethanol and acetonitrile, respectively, which are of higher relative polarity than dimethyl sulfoxide (DMSO),[78] in which a lower excitation energy of 2.74 eV was measured. It is emphasized that, in this study, we examined the theoretical results of the chromophores of interest in the gas phase, while, in future work, solvent properties will be studied in detail in comparison with systematic solution measurements.[79]

The ground-state dipole moment of 10.6 D, calculated with PBE0, is slightly larger than that calculated in previous studies, most of which overestimate the experimental value of 8.2 D in cyclohexane.[11,80] The dipole moment calculated for the first excited state, 26.1 D, is in better agreement with the 26.1 D value obtained in benzene[81] than with the 19.2 D value obtained in cyclohexane,[11,80] and mostly larger than those calculated previously (Table 1), except in a CNDO/S study,[5] which reported a value of 36.5 D. Therefore, the dipole difference we calculated, of 15.4 D, falls between the experimental values in cyclohexane (11 D) and benzene (19 D). The other key value for the calculation of the TPA cross section is the transition dipole moment. Except for the values from Das et al.[9] and Lapouyade et al.,[5] most of the transition dipole moments obtained theoretically, including in this work, are larger than the values of 7.1 D measured in cyclohexane, 7.4 D measured in DMSO, and 6.9−8.2 D measured in chloroform. However, this discrepancy is not surprising, since the calculations were carried out in the gas phase without the inclusion of any solvation effects.

In Table 2, we summarize the excitation energies and oscillator strengths calculated for each of the stilbene-based donor−acceptor compounds studied, as compared to the available experimental OPA spectra, measured in DMSO[12] and in cyclohexane.[8,77] For completeness, values measured in chloroform[82] are also included for ACCD and ANND. For ACCD, ACND, and ANCD, S1 is the charge-transfer state that corresponds to the measured peak, while, for ANND, aNND, and ANNd, S2 is the charge-transfer state. The PBE0 excitation energies are in good agreement with the excitation energies measured in cyclohexane for these molecules, and the B3LYP excitation energies are in fair agreement. The corresponding experimental oscillator strengths were not reported. However, for ANND, the oscillator strength (0.77) measured in chloroform,[82] a somewhat more polar solvent (with a dielectric constant of 4.81) than cyclohexane (dielectric constant of 2.02) but significantly less polar than DMSO (dielectric constant of 45.45), is in good agreement with the computed values (0.91 and 0.99). The good agreement of the PBE0 excitation energies with the spectra measured in cyclohexane are promising, in enabling the application to other materials in future studies. The

TABLE 2: Comparison of the Calculated Excitation Energies (eV) and Oscillator Strengths (*f*) for the First Two Excited States with Measured OPA Data for the Six Stilbene-Based A−D Compounds

	B3LYP		PBE0		experiment[a] (DMSO)[12]		experiment (cyclohexane)
molecule	energy	*f*	energy	*f*	energy	*f*	energy
ANNd							
S1	2.44	0.00	2.50	0.00			
S2	2.99	0.86	3.11	0.94	2.59	0.43	3.12[92]
aNND							
S1	2.52	0.00	2.55	0.00			
S2	2.99	1.09	3.07	1.13	2.64	0.58	
ANND							
S1	2.44	0.00	2.49	0.00			
S2	2.79	0.91	2.90	0.99	2.47	0.53[b]	2.79[92]
ANCD							
S1	3.06	0.62	3.24	0.76	2.98	0.50	3.26[8]
S2	3.73	0.32	3.85	0.13			
ACND							
S1	2.53	0.56	2.68	0.62	2.70	0.37	2.84[8]
S2	3.66	0.07	3.81	0.01			
ACCD							
S1	2.73	0.80	2.88	0.90	2.74	0.56[c]	2.98[8]
S2	3.76	0.00	3.84	0.00			

[a] Data have been obtained by digitization from spectra in cited reference and using a Gaussian line-shape. [b] The corresponding spectra obtained in chloroform:[82] Excitation energy of 2.58 eV and oscillator strength of 0.77 using a Gaussian line-shape. [c] In chloroform:[82] Excitation energy of 2.83 eV and oscillator strength of 0.73 using a Gaussian line-shape.

overestimation of the oscillator strengths may be attributed to the effects of solvent and may be partly due to the method of fitting the measured absorption data. Each absorption peak is fit to a Gaussian line-shape function, which may underestimate the oscillator strength. Previous theoretical studies on ACCD have reported oscillator strengths varying from 0.64 to 1.10, and therefore, the values of 0.8−0.9 found in this study are within that range and in good agreement with the observed value (0.73) in chloroform.[82]

The TPA spectra for the series of stilbene-based acceptor−donor molecules have been calculated using the two-state approximation, that is, including only the ground state and the first excited state in the SOS (eq 12), requiring the first-excited-state energy, the transition dipole moment between the ground state and the first excited state, and the dipoles for both the ground state and the first excited state. When eq 12 is used to obtain the TPA cross section at the maximum of the line-shape function (corresponding to half of the transition energy), the excitation energy is not included but the line width and form of the line-shape function must be determined. Both Gaussian and Lorentzian line-shape functions were used, with the widths obtained from the experimental TPA spectra.[12]

The TPA cross sections calculated for the six donor−acceptor compounds using eq 12 are listed in Table 3. The line width (fwhm), in eV, is the full width at half-maximum for the TPA transition. In Figure 3, the measured and calculated TPA spectra are shown over the range of photon energies from 1 to 2 eV (1240−620 nm). As defined in eq 12, the energies listed in Table 3 for the TPA peak correspond to half of the transition energy. Since in Figure 3 the cross section is given as a function of photon energy, the width of the plotted spectral lines is half of the fwhm of the TPA transition energy. The experimentally measured position and magnitude of the peak TPA cross section for each of these compounds, as given by Antonov et al.,[12] are also listed in Table 3. In addition, the transition dipole moments have been extracted from the oscillator strengths obtained in the experimental study,[12] and experimental values for the ground- and excited-state dipole moments are also available for four of these compounds,[81] allowing for the calculation of the cross section by the two-state approximation from experimental quantities. These results are given for both Gaussian and Lorentzian line-shape functions.

TABLE 3: Peak TPA Absorption Energies and Cross Sections Calculated Using TDDFT and the Two-State Approximation with the Indicated Line-Shape Function in Comparison to Experimental Values[a]

		B3LYP		PBE0		experiment[12]	
	fwhm (eV)	*E* (eV)	*δ* (GM)	*E* (eV)	*δ* (GM)	*E* (eV)	*δ* (GM)
ANNd		1.49		1.55		1.31	118
Gaussian	0.40		123		112		
Lorentzian	0.40		84		76		
aNND		1.49		1.53		1.31	77
Gaussian	0.48		50		53		
Lorentzian	0.48		34		36		
ANND		1.39		1.45		1.27	178
Gaussian	0.38		176		165		269[b]
Lorentzian	0.38		119		112		183[b]
ANCD		1.53		1.62		1.41	76
Gaussian	0.62		195		188		97[b]
Lorentzian	0.62		132		128		66[b]
ACND		1.26		1.34		1.32	133
Gaussian	0.42		235		242		146[b]
Lorentzian	0.42		160		164		99[b]
ACCD		1.37		1.44		1.36	191
Gaussian	0.52		215		222		231[b]
Lorentzian	0.52		146		151		156[b]

[a] For the three NN compounds, the second excited state was used in the two-state model. [b] Experimental dipole moments and transition moments were used to calculate TPA cross section by the two-state approximation (see text).

The calculated TPA cross section is in good agreement with the peak experimental value for ACCD, using the experimental two-state approximation, where the two values (from Gaussian and Lorentzian line-shapes) bracket the measured maximum cross section, indicating that if an appropriately hybridized line-shape function could be applied, the two-state approximation would result in good agreement with the measured peak. The measured peak cross section for ACCD (191 GM)[12] also is in good agreement with that reported previously for a similar molecule (with dibutyl amino as the donor group) using picosecond Kerr ellipsometry (170 GM).[83] In that study, a TPA cross section of 102 GM[83] was reported for (2-hydroxyethyl-ethyl)-amino-nitroazobenzene, which is close to the femtosecond *Z*-scan result for ANNd (118 GM)[12] listed in Table 3.

The TPA cross sections calculated using B3LYP with the Gaussian and Lorentzian line-shapes for ACCD underestimate the corresponding experimentally derived cross sections by 7%, while the PBE0 calculated cross sections underestimate the experimental values by just 4%. However, this good agreement is the result of some cancellation of errors: while the calculated transition dipole moments are 19% (B3LYP) and 23% (PBE0) larger than experiment, the dipole differences are 19% (B3LYP) and 20% (PBE0) less than experiment. Our calculated transition dipole moments are consistently larger than the measured values, as indicated by the values of the oscillator strengths in Table 2, and this is the primary reason that our calculated TPA cross sections are larger than the measured values, particularly for the two hybrid compounds. These deviations could result from a comparison with the experimental spectra measured in DMSO. For the azo compounds, there is some cancellation of error, and our TPA cross sections using a Gaussian line-shape are in fairly good agreement with experiment. For ANND, both two-state approximations are larger than the measured cross section,

a) ANNd (DO3)

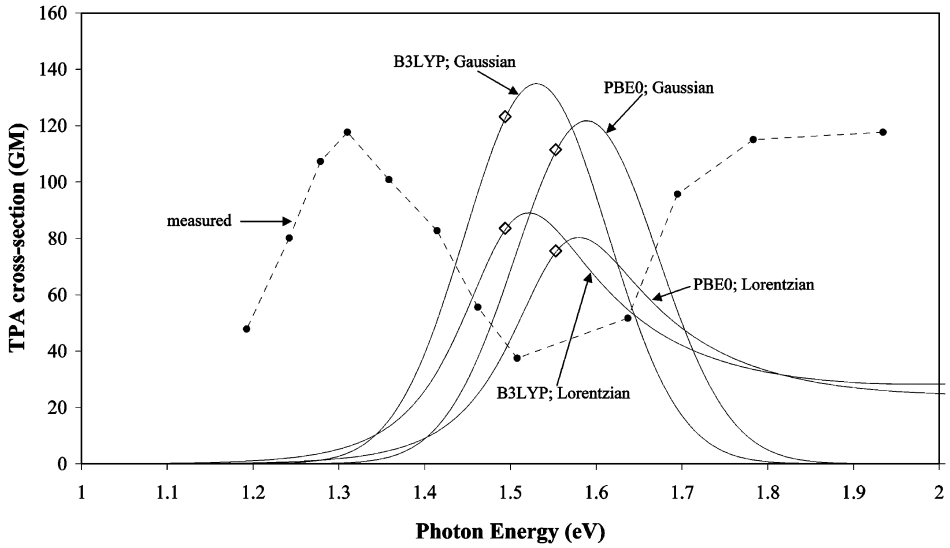

b) aNND

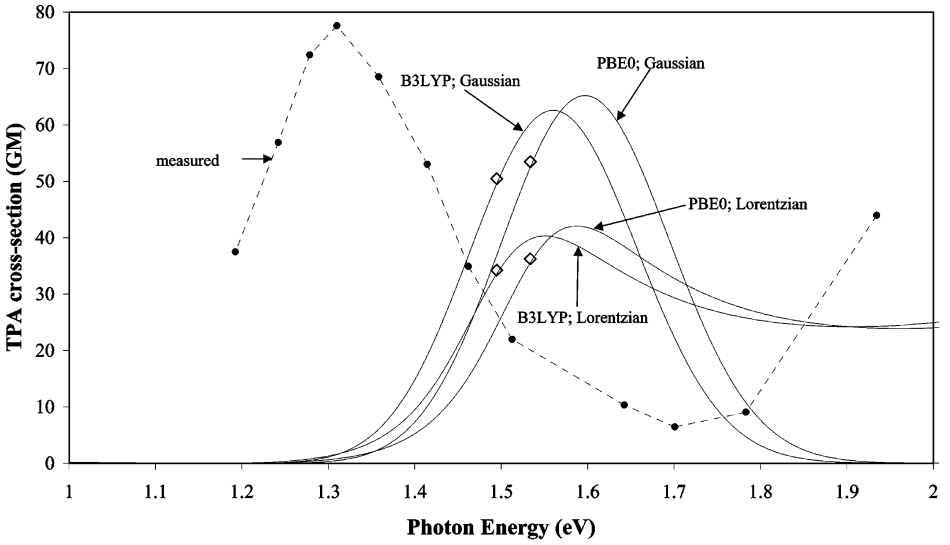

c) ANND

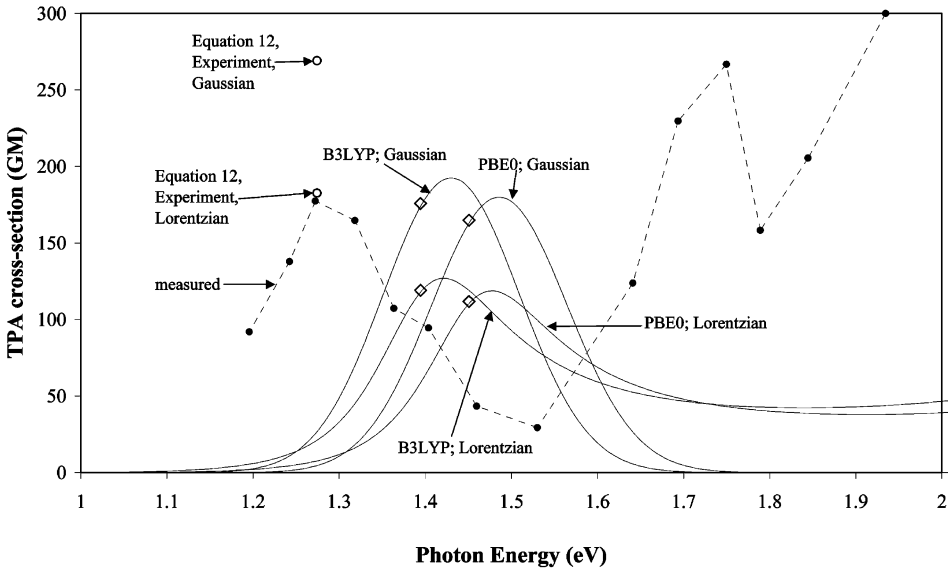

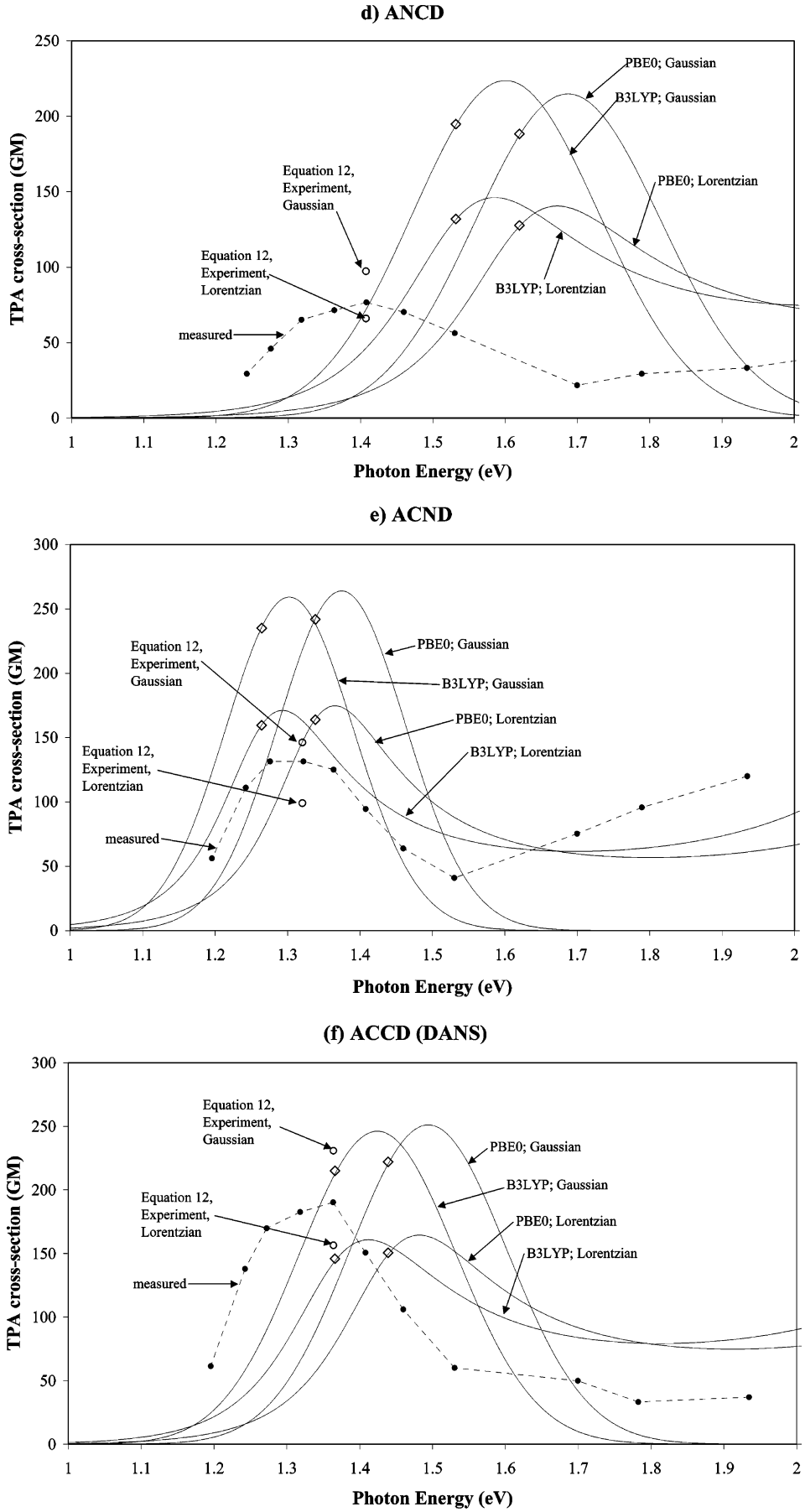

Figure 3. TPA cross sections for the stilbene-based D−A compounds as a function of photon energy. Each curve was calculated using eq 7 with the indicated (x-c) functional and line-shape, while each diamond indicates the peak TPA cross section calculated with eq 12. The experimental data is from Antonov et al.[12]

TABLE 4: Computed OPA Excitation Energies (eV) and Oscillator Strengths (*f*) for Fluorene Compared to Experimental Results

		PBE0		B3LYP		SAC-CI		experiment[a]	
state	basis set	energy	*f*	energy	*f*	energy	*f*	energy	*f*
1^1B_2	6-311++G(d,p)	4.57	0.199	4.45	0.159	4.78	0.167	4.12	0.015
	6-31G(d)			4.68	0.175	4.89	0.062		
2^1B_2	6-311++G(d,p)	4.76	0.252	4.64	0.282	5.15	0.485	4.75	0.337
	6-31G(d)			4.79	0.245	5.45	0.443		
1^1A_1	6-311++G(d,p)	4.91	0.008	4.81	0.007	5.16	0.008		
	6-31G(d)			4.93	0.007	5.09	0.004		

[a] The data have been obtained by digitization from spectrum in isooctane.[84] The corresponding spectra in cyclohexane:[95] [4.12 ($f = 0.022$), 4.19 (shoulder), 4.30, 4.72, 4.75 ($f = 0.391$)].

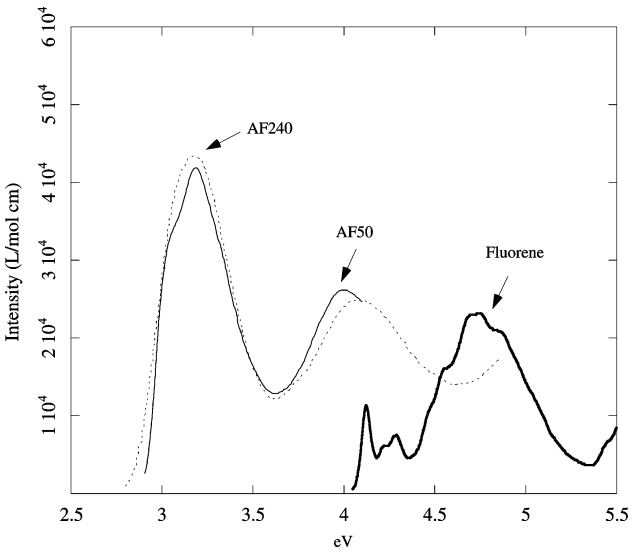

Figure 4. Experimental OPA spectra of fluorene[95] (in cyclohexane), AF50[15] (in hexane), and AF240[69] (in THF).

indicating that other terms in the SOS are likely to be important, while, for aNND and ANNd, good agreement with experiment by applying a Gaussian line-shape function is noted.

Note that, in the broadband TPA spectra given in Figure 3, each of the cross section functions plotted using eqs 7−10 with the two-state approximation has a maximum at a slightly higher energy than the "theoretical maximum", calculated using eq 12. In eq 12, we assume the photon energy is half of the TPA state energy (the maximum of the Gaussian or Lorentzian line-shape function), while eq 7 peaks at a different value due to the energy dependence in the rest of the function, which is proportional to

$$\left(1 - \frac{\mu_{ff}}{\mu_{00}}\left[\frac{E_\lambda}{E_f - E_\lambda}\right]\right)^2$$

For the molecules studied, the difference in the maximum of the TPA cross section function, defined by using two states in eqs 7−10, and the TPA cross section at the TPA resonance energy, defined by eq 12, is small, but for ACCD (Figure 3f), the former is larger than the experimentally derived value, while the latter is less than experiment.

3.B. Fluorene-Based Donor−Acceptor (AFX) Molecules. We first report the calculated and measured excitation energies and oscillator strengths for fluorene (Table 4). The low-energy absorption spectrum of fluorene (Figure 4) has three groups of bands with maxima at 4.12 ($f = 0.053$), 4.29, and 4.75 eV ($f = 0.337$). The lowest transition has been assigned the electronic state 1^1B_2.[84,85] Two-photon data obtained by Drucker and McClain[86] also indicate that the first transition (4.23 eV in benzene) is of B_2 symmetry. The SAC-CI and TDDFT calculations agree that the first excited state is of B_2 symmetry with small oscillator strength. The gas-phase TDDFT/6-311++G(d,p) calculation overestimates the excitation energy relative to the experimental results in solution by 0.33 (B3LYP) and 0.45 (PBE0) eV, while the corresponding SAC-CI energy computed with the same basis set is ∼0.66 eV larger than experiment. Notably, both the computed SAC-CI and TDDFT oscillator strengths are in good agreement with experiment, with TDDFT underestimating the strength of the strongest transition (2^1B_2) by ∼0.06 and SAC-CI overestimating it by ∼0.15. The TDDFT overestimation of the excitation energy is larger that than that observed for the stilbene-based molecules (Table 2), possibly due to a comparison with an experimental measurement in a different solvent. SAC-CI transition dipoles are more basis set sensitive. TDDFT predicts the second (4.76 eV) and third (4.81 eV) excited states to have B_2 and A_1 symmetries. These two SAC-CI states are almost degenerate. Thus, the strong transition observed at 4.75 eV can be attributed to the 2^1B_2 electronic state. The TPA spectrum in cyclohexane also indicates a peak at 4.72 eV.[86] The absolute TPA cross section was not reported. Since the computed SAC-CI and TDDFT dipole moments for the ground and first three excited states are small, the TPA cross section for fluorene is likely to be primarily from type I TPA, and thus, the two-state approximation would not be appropriate.

The substitutions of the donor and acceptor in fluorene resulted in the loss of C_{2v} symmetry. Although the AF molecules have C_1 symmetry, unconstrained (Newton−Raphson) optimization does not necessarily lead to the lowest energy structure. As expected, the AF structures with linear anti straight-chain dialkyl groups are found to be lower in energy compared to other *n*-alkyl analogues. In these structures, the phenyl rings of the diphenylamine group are not coplanar with or orthogonal to the fluorene plane. The vicinal (opposite) phenyl of the *n*-alkyl groups rotates about −45° (−40°) out of the fluorenyl plane. Note that the corresponding positive rotations of the phenyl groups produce AFX sterioisomers. For AF240, benzothiazol substitution having sulfur opposite to the diethyl group resulted in slightly lower energy compared to the corresponding gauche arrangement. We consider the lowest energy structure of the AFX molecules in the discussion below, unless mentioned otherwise.

In Table 5, we show, similar to the results obtained for the stilbene-based molecules, that B3LYP consistently underestimates the excitation energy in comparison with that obtained with the PBE0 (x-c) functional. We find a mean absolute deviation (MAD) of 0.14 eV between the two functionals for the first five excited states. However, the differences in the oscillator strengths predicted by the two functionals are small, with a MAD of <0.1. Although numerous examples show the B3LYP excitation energies and the oscillator strengths to compare favorably with experiments, the PBE0 excitation energies are clearly in better agreement (cf. Tables5 and 6).

TABLE 5: Computed OPA Results for B3LYP and PBE0 Functionals for AFX Molecules

	6-31G(d)				6-311G(d,p)			
molecule	PBE0 energy	*f*	B3LYP energy	*f*	PBE0 energy	*f*	B3LYP energy	*f*
AF50[a]								
2^1A	2.96 (2.95)	1.021 (0.987)	2.82 (2.81)	0.880 (0.854)	2.95	1.024	2.80	0.883
3^1A	3.86 (3.85)	0.811 (0.718)	3.71 (3.70)	0.894 (0.799)	3.77	0.028	3.62	0.084
4^1A	3.89 (3.87)	0.025 (0.058)	3.76 (3.74)	0.047 (0.078)	3.83	0.771	3.68	0.821
5^1A	4.06 (4.04)	0.026 (0.021)	3.92 (3.90)	0.013 (0.009)	3.99	0.032	3.85	0.020
6^1A	4.13 (4.12)	0.203 (0.197)	4.00 (3.99)	0.185 (0.180)	4.06	0.190	3.93	0.174
AF240[b]								
2^1A	3.05 (3.04)	0.991 (0.949)	2.91 (2.91)	0.887 (0.849)	3.04	1.002	2.90	0.898
3^1A	3.90 (3.90)	0.010 (0.011)	3.76 (3.76)	0.025 (0.030)	3.78	0.008	3.64	0.009
4^1A	3.96 (3.96)	0.545 (0.528)	3.82 (3.81)	0.619 (0.595)	3.95	0.509	3.80	0.592
5^1A	4.14 (4.14)	0.199 (0.197)	4.01 (4.01)	0.180 (0.174)	4.05	0.186	3.92	0.174
6^1A	4.19 (4.19)	0.039 (0.039)	4.04 (4.04	0.028 (0.034)	4.13	0.028	3.98	0.018

[a] Methyl analogue of AF50. Results for the full AF50 molecule, which has decyl pendants, are in parentheses. [b] Results for AF69 (decyl analogue of AF240) are in parentheses.

TABLE 6: TD-PBE0/6-31G(d) OPA Excitation Energies (eV) and Oscillator Strengths (*f*) Compared with Other Calculations[a] and with Experimental Results

	theory		experiment			
molecule	energy	*f*	energy	*f*	solvent	ref
AF50						
2^1A	2.96	0.950	3.19[b]	0.642[b]	hexane	15
			3.21		PMMA	96
			3.18		THF	69
			3.20	1.45[b]	THF	97
3^1A	3.85	0.758	4.00[b]	0.775[b]	hexane	15
			4.06		THF	98
			3.87		benzene	99
AF50P						
2^1A	2.95	1.263	3.24		CH3CN	91
3^1A	3.76	0.892	4.03		CH3CN	91
4^1A	3.87	0.007				
5^1A	4.01	0.032				
6^1A	4.12	0.199				
AF240						
2^1A	3.05	0.991	3.08		hexane	100
			3.17[b]	0.657[b]	THF	69
			3.15	0.479[b]	THF	87
			3.15	0.708[b]	toluene	87
4^1A	3.96	0.545	4.04		hexane	100
			3.99[b]	0.616[b]	THF	69
			3.91		THF	87
AF69[c]						
2^1A	3.04	0.949	3.02		hexane	101
			3.16		THF	89
3^1A	3.90	0.011				
4^1A	3.96	0.528	4.07		hexane	101
5^1A	4.14	0.197				
6^1A	4.19	0.039				

[a] Excitation energy and oscillator strength (*f*) for AF50: 3.57 (1.625) from INDO/S CI//AM1 for the methyl analogue;[15] 3.03 from AM1 CI for the methyl analogue;[9] and 4.10 (1.53), 5.05 (0.05), 5.22 (0.11), and 5.31 (0.11) from RPA//AM1 for the methyl analogue.[16] Excitation energy and oscillator strength (*f*) for AF240: 2.86 (0.907) from TD-B3LYP/6-31G(d,p)//B3LYP/6-31G(d,p).[17] [b] The data have been obtained by digitization from the spectrum in the cited reference. The experimental oscillator strengths were computed using eq 3. [c] Decyl analogue of AF240.

The TDDFT method was found to overestimate the oscillator strength for the first excited state by ~30% (B3LYP) or ~50% (PBE0), while the calculated oscillator strengths for the second strongly allowed transition are in good agreement with experiment. For the two diphenylaminofluorene-based chromophores studied, the excitation energies obtained with PBE0/6-31G(d) were found to be in good agreement with experiment, with a mean error of 0.14 eV. We find the largest deviation of 0.23 eV for AF50. Once again, it is encouraging that good agreement with experimental spectra measured in hexane is obtained, for example, for AF69 and AF240, while for AF50 the trend is well reproduced.

TABLE 7: Computed TPA Results for B3LYP and PBE0 Functionals Using a Gaussian Line-Shape Function and the 6-31G(d) Basis Set[a]

	PBE0		B3LYP		
molecule	δ (GM)	$\Delta\mu$ (D)	δ (GM)	$\Delta\mu$ (D)	fwhm[b] (eV)
AF50					
2^1A	819	20.6	872	22.3	0.28[102]
AF50[c]					
2^1A	880 (857)	21.0 (20.6)	915 (910)	22.8 (22.3)	0.28[102]
AF50P					
2^1A	659	20.9	727	23.1	0.46[91]
AF240					
2^1A	774 (727)	17.6 (16.9)	845 (809)	19.0 (18.4)	0.21[87]
AF69[d]					
2^1A	336	17.7	371	19.2	0.47[88]

[a] The values in parentheses were computed with the 6-311G(d,p) basis set. [b] The data have been obtained by digitization from the spectrum in the cited reference. [c] Methyl analogue of AF50. [d] Decyl analogue of AF240.

The computed B3LYP and PBE0 TPA cross sections are listed in Table 7. These computed values were obtained with the two-state approximation (eq 12) using the Gaussian line shape (eq 8). The corresponding values using a Lorentzian line shape are obtained by dividing by 1.48. The fwhm for each system was obtained from the corresponding experimental TPA spectrum. Previous computed and experimental TPA cross sections are included in Table 8 for comparison.

The OPA spectrum of AF50 has been reported for a number of solvents. The spectrum from 300 to 400 nm exhibits two broad bands. In hexane, the low-energy band reveals a shoulder at ~3.0 eV in addition to a maximum at 3.19 eV. Their combined oscillator strengths are ~0.64 (Gaussian fit). TDDFT predicts a single transition at 2.96 eV with an oscillator strength of 0.95 in this region. Thus, the maximum at 3.19 eV is likely vibronic in nature. Our computed results for the low-energy band are in good agreement with previous AM1-CI[9] results for the methyl analogue (Table 6). The computed INDO/S[15] and RPA[16] excitation energies and oscillator strengths, however, are significantly larger than the corresponding TDDFT and experimental values (Table 6). The first excited state of AF50 exhibits strong TPA, simultaneously absorbing two photons when the photon energy is half of the transition energy. Experimentally, TPA is reported to occur at ~1.56-1.59 eV and TPA cross sections in the range 22−800 GM have been reported. The calculated cross sections for AF50 also vary widely. Das et al.[9]

TABLE 8: TD-PBE0/6-31G(d) TPA Excitation Energies (eV) and Cross Sections (δ) (cm^4 photon^{-1} s) Compared with Other Calculations[a] and with Experimental Results[b]

	theory		experiment				
molecule	energy	δ (GM)	energy	δ (GM)	method	solvent	ref
AF50							
2^1A	1.41	819	1.56	30	*Z*-scan	benzene	99
			1.59	166	DFWM	acetone	102
			1.56	22	*Z*-scan	THF	98
			1.61	56	WLC	THF	97
			1.57	25	*Z*-scan	benzene	103
			1.59	800	TPF	PMMA	96
AF50P							
2^1A	1.48	660	1.54	650	WLC	CH_3CN	91
AF240							
2^1A	1.52	774	1.51	150	TPF	THF	87
AF69							
2^1A	1.52	336	1.52	820	WLC	THF	89
			1.59	100	*Z*-scan	THF	90
			1.60	120	WLC	THF	90

[a] **AF50**-RPA/6-31G//AM1 for the methyl analogue using Lorentzian line-shape with a fwhm of 0.2 eV, 142 GM;[16] AM1 CI for the methyl analogue using Gaussian line-shape with a fwhm of 0.21 eV, 56 GM.[9] CIS using Lorentzian line-shape with a fwhm of 0.2 eV, 370 GM.[104] **AF240**-TD-B3LYP/6-31G(d,p)//B3LYP/6-31G(d,p) using Lorentzian line-shape with a fwhm of 0.2 eV, 1240 GM (856 GM using Gaussian line-shape with a fwhm of 0.21 eV and a correction factor of $^1/_2$ for direct comparison with experiment).[17] [b] The experimental energies listed correspond to the photon energy in degenerate experiments, or to half of the sum of the photon energies in nondegenerate experiments, such as the white light continuum (WLC).

reported a TPA cross section of 56 GM (this value needs to be scaled by a factor of π for direct comparison with our computed values) using AM1-CI, while Wang et al.[16] reported a computed RPA/6-31G cross section of 142 GM (this value needs to be scaled by a factor of 0.5 for direct comparison with our computed values) for the AF50 ethyl analogue. The computed TDDFT TPA cross section is about 5 times larger than the AM1-CI value and about 11 times larger than the RPA value. The large discrepancy between TDDFT and RPA is consistent with the recent results reported by Guo et al. for other AF chromophores.[17]

Similar to AF50, the OPA spectrum of AF240 taken in tetrahydrofuran (THF) has two broad bands. In hexane, the low-energy one splits into two peaks located at 3.05 and 3.22 eV. The latter is assigned to a vibronic progression based upon the computed results. The next band is broad and featureless in both THF and hexane. There are several electronic transitions that may contribute to this broad band at ~4 eV (see Tables 5 and 6). The transition at 3.95 eV with an oscillator strength of 0.56 is predicted to have a dominant contribution to the intensity of this high-energy band. The computed oscillator strength is in good agreement with the experimental value obtained in THF. Theory, however, overestimates the intensity of the low-energy band. Note that the computed B3LYP/6-31G(d) energy and oscillator strength for the first excited state are almost identical to the B3LYP/6-31G(d,p) values reported by Guo et al.,[17] predicting a TPA cross section of 1240 GM for the first excited state using a Lorentzian line-shape with a fwhm of 0.20 eV. This corresponds to a TPA cross section of 620 GM using our convention (eqs 5−7). We calculated a TPA cross section of 845 GM using a Gaussian line-shape with a fwhm of 0.21 eV, but if we use a Lorentzian line-shape with a fwhm of 0.20, we obtain a TPA cross section of 601 GM, which is only 3% lower than the result of Guo et al.[17] Although it is encouraging that the theoretical results are consistent, the discrepancy with experiment is to be further investigated. The computed TDDFT cross sections are more than 5 times the peak cross section (150 GM) measured in THF.[87]

The calculated OPA spectrum for AF69, the decyl analogue of AF240, is similar to AF240, and good agreement with experiment is obtained. Since the two key values in our calculation of the TPA cross section, the transition dipole moment and the dipole difference, are similar for these two molecules, we expect to calculate similar TPA cross sections. However, the TPA line width found for AF69[88] is more than twice the line width found for AF240,[87] so our calculated cross section of AF69 is half that calculated for AF240. While increased vibrational broadening in AF69 due to the larger alkyl pendants is not unexpected, the factor of 2 increase in line width is surprising, underlining the need for an independent theoretical method for obtaining the line width in order to predict TPA cross sections a priori. While the experimental value for the AF240 TPA cross section is 150 GM, for AF69, values of 100, 120, and 820 GM have been reported. Thus, our calculated TPA cross section is less than half of the earlier reported value[89] and more than 3 times the more recent experimental values.[90]

The calculated OPA spectrum for AF50P appears to underestimate the energies of each of the first two peaks by ~0.3 eV. However, the calculated TPA cross section is in excellent agreement with experiment. Because of the wide range of measured TPA cross sections that have been reported for AF50, the relative TPA strength of these two molecules cannot be assessed experimentally. While for AF50P we calculated a larger transition dipole moment than for AF50, due to the larger line width obtained for AF50P,[91] the calculated peak TPA cross section is ~20% less than that calculated for AF50.

4. Conclusions

OPA and TPA properties have been calculated for D−π−A compounds using TDDFT, showing that the PBE0 (x-c) functional gave more accurate values for both the stilbene-based and the fluorene-based compounds. However, an overestimation of the oscillator strengths, in comparison to experiment, was noted in some cases. Because of the wide spread in experimentally measured TPA cross sections and the lack of experimental systematic solvatochromic-shift studies, the accuracy of the two-state approximation in estimating the TPA cross sections cannot yet be accurately assessed. Also, the experimentally derived line widths used in the calculation of the peak TPA cross section introduced an undesirable variability in our calculated values. A careful investigation, in collaboration with Rogers et al. (e.g., for AF270)[79] in future work, would enable a more accurate assessment, while calculations for small model compounds may highlight required developments.

Acknowledgment. This research has been supported by the Air Force Office of Scientific Research (AFOSR) and by CPU time from the Aeronautical Systems Center (ASC) Major Shared Resource Center (MSRC). We gratefully acknowledge useful discussions with Drs. Joy Rogers, Loon-Seng Tan, and Richard Sutherland from AFRL.

Supporting Information Available: Coordinates of all optimized molecular structures. This material is available free of charge via the Internet at http://pubs.acs.org.

References and Notes

(1) Dvornikov, A. S.; Rentzepis, P. M. *Science* **1989**, *245*, 843.
(2) Denk, W.; Strickler, J. H.; Webb, W. W. *Science* **1990**, *248*, 73.

(3) Bhawalkar, J. D.; He, G. S.; Prasad, P. N. *Rep. Prog. Phys.* **1996**, *59*, 1041.
(4) Albota, M.; Beljonne, D.; Bredas, J. L.; Ehrlich, J. E.; Fu, J. Y.; Heikal, A. A.; Hess, S. E.; Kogej, T.; Levin, M. D.; Marder, S. R.; McCord-Maughon, D.; Perry, J. W.; Rockel, H.; Rumi, M.; Subramaniam, G.; Webb, W. W.; Wu, X. L.; Xu, C. *Science* **1998**, *281*, 1653.
(5) Lapouyade, R.; Kuhn, A.; Letard, J.-F.; Rettig, W. *Chem. Phys. Lett.* **1993**, *208*, 48.
(6) Morley, J. O. *J. Phys. Chem.* **1994**, *98*, 13182.
(7) Beljonne, D.; Bredas, J. L.; Cha, M.; Torruellas, W. E.; Stegeman, G. I.; Hofstraat, J. W.; Horsthuis, W. H. G.; Mohlmann, G. R. *J. Chem. Phys.* **1995**, *103*, 7834.
(8) van Walree, C. A.; Franssen, O.; Marsman, A. W.; Flipse, M. C.; Jenneskens, L. W. *J. Chem. Soc., Perkin Trans.* **1997**, *2*, 799.
(9) Das, G. P.; Yeates, A. T.; Dudis, D. S. *J. Opt. Soc. Am. B* **1997**, *14*, 2325.
(10) Das, G. P.; Dudis, D. S. *Chem. Phys. Lett.* **1999**, *312*, 57.
(11) Farztdinov, V. M.; Ernsting, N. P. *Chem. Phys.* **2002**, *277*, 257.
(12) Antonov, L.; Kamada, K.; Ohta, K.; Kamounah, F. *Phys. Chem. Chem. Phys.* **2003**, *5*, 1193.
(13) DeBoni, L.; Rodrigues, J. J., Jr.; dos Santos, D. S., Jr.; Silva, C. H. T. P.; Balogh, D. T.; Oliveira, O. N., Jr.; Zilio, S. C.; Misoguti, L.; Mendonca, C. R. *Chem. Phys. Lett.* **2002**, *361*, 209.
(14) Rumi, M.; Ehrlich, J. E.; Heikal, A. A.; Perry, J. W.; Barlow, S.; Hu, Z.; McCord-Maughon, D.; Parker, T. C.; Rockel, H.; Thayumanavan, S.; Marder, S. R.; Beljonne, D.; Bredas, J.-L. *J. Am. Chem. Soc.* **2000**, *122*, 9500.
(15) Baur, J. W.; Alexander, M. D., Jr.; Banach, M.; Denny, L.; Reinhardt, B. A.; Vaia, R. A.; Fleitz, P. A.; Kirkpatrick, S. M. *Chem. Mater.* **1999**, *11*, 2899.
(16) Wang, C.-K.; Macak, P.; Agren, H. *J. Chem. Phys.* **2001**, *114*, 9813.
(17) Guo, J.-D.; Wang, C.-K.; Luo, Y.; Agren, H. *Phys. Chem. Chem. Phys.* **2003**, *5*, 3869.
(18) Nguyen, K. A.; Kennel, J.; Pachter, R. *J. Chem. Phys.* **2002**, *117*, 7128.
(19) Nguyen, K. A.; Pachter, R. *J. Chem. Phys.* **2003**, *118*, 5802.
(20) Nguyen, K. A.; Day, P. N.; Pachter, R.; Tretiak, S.; Chernyak, V.; Mukamel, S. *J. Phys. Chem. A* **2002**, *106*, 10757.
(21) Day, P. N.; Nguyen, K. A.; Pachter, R. First Principle Calculations of Two-Photon Absorption Spectra: Trans-Octatetraene and Trans-Stilbene. Proceedings of SPIE 4797: Multiphoton Absorption and Nonlinear Transmission Processes: Materials, Theory, and Applications, Seatle, WA, 2003.
(22) Furche, F. *J. Chem. Phys.* **2001**, *114*, 5982.
(23) Salek, P.; Vahtras, O.; Guo, J.; Luo, Y.; Helgaker, T.; Agren, H. *Chem. Phys. Lett.* **2003**, *374*, 446.
(24) Baev, A.; Gel'mukhanov, F.; Rubio-Pons, O.; Cronstrand, P.; Agren, H. *J. Opt. Soc. Am. B* **2004**, *21*, 384.
(25) Kong, J.; White, C. A.; Krylov, A. I.; Sherrill, C. D.; Adamson, R. D.; Furlani, T. R.; Lee, M. S.; Lee, A. M.; Gwaltney, S. R.; Adams, T. R.; Ochsenfeld, C.; Gilbert, A. T. B.; Kedziora, G. S.; Rassolov, V. A.; Maurice, D. R.; Nair, N.; Shao, Y.; Besley, N. A.; Maslen, P. E.; Dombroski, J. P.; Dachsel, H.; Zhang, W. M.; Korambath, P. P.; Baker, J.; Byrd, E. F. C.; Voorhis, T. V.; Oumi, M.; Hirata, S.; Hsu, C. P.; Ishikawa, N.; Florian, J.; Warshel, A.; Johnson, B. G.; Gill, P. M. W.; Head-Gordon, M.; Pople, J. A. *Q-Chem*, 2.0 ed.; Q-Chem, Inc.: Export, PA, 2000.
(26) Bartholomew, G. P.; Rumi, M.; Pond, S. J. K.; Perry, J. W.; Tretiak, S.; Bazan, G. C. *J. Am. Chem. Soc.* **2004**, *126*, 11529.
(27) Masunov, A. M.; Tretiak, S. *J. Phys. Chem. B* **2004**, *108*, 899.
(28) Morel, Y.; Irimia, A.; Najechalski, P.; Kervella, Y.; Stephan, O.; Baldeck, P. L. *J. Chem. Phys.* **2001**, *114*, 5391.
(29) Das, G. P.; Vaia, R.; Yeates, A. T.; Dudis, D. S. *Synth. Met.* **2001**, *116*, 281.
(30) Sheik-Bahae, M.; Said, A. A.; Wei, T. H.; Hagan, D. J.; Stryland, E. W. V. *IEEE J. Quantum Electron.* **1990**, *26*, 760.
(31) Karotki, A.; Drobizhev, M.; Dzenis, Y.; Taylor, P. N.; Anderson, H. L.; Rebane, A. *Phys. Chem. Chem. Phys* **2004**, *7*, 7.
(32) Dierksen, M.; Grimme, S. *J. Chem. Phys.* **2004**, *120*, 3544.
(33) Macak, P.; Luoa, Y.; Norman, P.; Ågren, H. *J. Chem. Phys.* **2000**, *113*, 7055.
(34) Boldrini, B.; Cavalli, E.; Painelli, A.; Terenziani, F. *J. Phys. Chem. A* **2002**, *106*, 6286.
(35) Kohn, W.; Sham, L. J. *Phys. Rev. A* **1965**, *140*, 1133.
(36) McLean, A. D.; Chandler, G. S. *J. Chem. Phys.* **1980**, *72*, 5639.
(37) Krishnan, R.; Binkley, J. S.; Seeger, R.; Pople, J. A. *J. Chem. Phys.* **1980**, *72*, 650.
(38) Ditchfield, R.; Hehre, W. J.; Pople, J. A. *J. Chem. Phys.* **1971**, *54*, 724.
(39) Hehre, W. J.; Ditchfield, R.; Pople, J. A. *J. Chem. Phys.* **1972**, *56*, 2257.
(40) Becke, A. D. *J. Chem. Phys.* **1993**, *98*, 5648.
(41) Becke, A. D. *Phys. Rev. A* **1988**, *38*, 3098.
(42) Lee, C.; Yang, W.; Parr, R. G. *Phys. Rev. B* **1988**, *37*, 785.
(43) Vosko, S. H.; Wilk, L.; Nusair, M. *Can. J. Phys.* **1980**, *58*, 1200.
(44) Stephens, P. J.; Devlin, F. J.; Chabalowski, C. F.; Frisch, M. J. *J. Phys. Chem.* **1994**, *98*, 11623.
(45) Bauernschmitt, R.; Ahlrichs, R. *Chem. Phys. Lett.* **1996**, *256*, 454.
(46) Casida, M.; Jamorski, C.; Casida, K. C.; Salahub, D. R. *J. Chem. Phys.* **1998**, *108*, 4439.
(47) Stratmann, R. E.; Scuseria, G. E.; Frisch, M. J. *J. Chem. Phys.* **1998**, *109*, 8218.
(48) Frisch, M. J.; Trucks, G. W.; Schlegel, H. B.; Scuseria, G. E.; Robb, M. A.; Cheeseman, J. R.; Zakrzewski, V. G.; Montgomery, J. A.; Stratmann, R. E.; Burant, J. C.; Dapprich, S.; Millam, J. M.; Daniels, A. D.; Kudin, K. N.; Strain, M. C.; Farkas, O.; Tomasi, J.; Barone, V.; Cossi, M.; Cammi, R.; Mennucci, B.; Pomelli, C.; Adamo, C.; Clifford, S.; Ochterski, J.; Petersson, G. A.; Ayala, P. Y.; Cui, Q.; Morokuma, K.; Malick, D. K.; Rabuck, A. D.; Raghavachari, K.; Foresman, J. B.; Cioslowski, J.; Ortiz, J. V.; Baboul, A. G.; Stefanov, B. B.; Liu, G.; Liashenko, A.; Piskorz, P.; Komaromi, I.; Gomperts, R.; Martin, R. L.; Fox, D. J.; Keith, T.; Al-Laham, M. A.; Peng, C. Y.; Nanayakkara, A.; Gonzalez, C.; Challacombe, M.; Gill, P. M. W.; Johnson, B. G.; Chen, W.; Wong, M. W.; Andres, J. L.; Head-Gordon, M.; Replogle, E. S.; Pople, J. A. *Gaussian 98*, revision A.11.4; Gaussian, Inc.: Pittsburgh, PA, 2000.
(49) Frisch, M. J.; Trucks, G. W.; Schlegel, H. B.; Scuseria, G. E.; Robb, M. A.; Cheeseman, J. R.; Montgomery, J. A., Jr.; Vreven, T.; Kudin, K. N.; Burant, J. C.; Millam, J. M.; Iyengar, S. S.; Tomasi, J.; Barone, V.; Mennucci, B.; Cossi, M.; Scalmani, G.; Rega, N.; Petersson, G. A.; Nakatsuji, H.; Hada, M.; Ehara, M.; Toyota, K.; Fukuda, R.; Hasegawa, J.; Ishida, M.; Nakajima, T.; Honda, Y.; Kitao, O.; Nakai, H.; Klene, M.; Li, X.; Knox, J. E.; Hratchian, H. P.; Cross, J. B.; Adamo, C.; Jaramillo, J.; Gomperts, R.; Stratmann, R. E.; Yazyev, O.; Austin, A. J.; Cammi, R.; Pomelli, C.; Ochterski, J. W.; Ayala, P. Y.; Morokuma, K.; Voth, G. A.; Salvador, P.; Dannenberg, J. J.; Zakrzewski, V. G.; Dapprich, S.; Daniels, A. D.; Strain, M. C.; Farkas, O.; Malick, D. K.; Rabuck, A. D.; Raghavachari, K.; Foresman, J. B.; Ortiz, J. V.; Cui, Q.; Baboul, A. G.; Clifford, S.; Cioslowski, J.; Stefanov, B. B.; Liu, G.; Liashenko, A.; Piskorz, P.; Komaromi, I.; Martin, R. L.; Fox, D. J.; Keith, T.; Al-Laham, M. A.; Peng, C. Y.; Nanayakkara, A.; Challacombe, M.; Gill, P. M. W.; Johnson, B.; Chen, W.; Wong, M. W.; Gonzalez, C.; Pople, J. A. *Gaussian 03*, A.11.4 ed.; Gaussian, Inc.: Pittsburgh, PA, 2003.
(50) Ernzerhof, M.; Scuseria, G. E. *J. Chem. Phys.* **1999**, *110*, 5029.
(51) Adamo, C.; Scuseria, G. E. *J. Chem. Phys.* **1999**, *111*, 2889.
(52) Nakatsuji, H. *Chem. Phys. Lett.* **1978**, *59*, 362.
(53) Nakatsuji, H.; Hirao, K. *J. Chem. Phys.* **1978**, *68*, 2053.
(54) Nakatsuji, H. *Chem. Phys. Lett.* **1979**, *67*, 329.
(55) Nakatsuji, H. *Chem. Phys. Lett.* **1979**, *67*, 334.
(56) Goppert-Mayer, M. *Ann. Phys.* **1931**, *9*, 273.
(57) Sutherland, R. L. *Handbook of Nonlinear Optics*; Marcel Dekker: New York, 1996.
(58) Boyd, R. W. Multiphoton Absorption and Multiphoton Ionization. *Nonlinear Optics*, 2nd ed.; Academic Press: London, 2003; p 521.
(59) Peticolas, W. L. *Annu. Rev. Phys. Chem.* **1967**, *18*, 233.
(60) Masthay, M. B.; Findsen, L. A.; Pierce, B. M.; Bocian, D. F.; Lindsey, J. S.; Birge, R. R. *J. Chem. Phys.* **1986**, *84*, 3901.
(61) Birge, R. R.; Zhang, C.-F. *J. Chem. Phys.* **1990**, *92*, 7118.
(62) Poulsen, T. D.; Frederiksen, P. K.; Jorgensen, J.; Mikkelsen, K. V.; Ogilby, P. R. *J. Phys. Chem. A* **2001**, *105*, 11488.
(63) Shima, S.; Ilagan, R. P.; Gillespie, N.; Sommer, B. J.; Hiller, R. G.; Sharples, F. P.; Frank, H. A.; Birge, R. R. *J. Phys. Chem. A* **2003**, *107*, 8052.
(64) Monson, P. R.; McClain, W. M. *J. Chem. Phys.* **1970**, *53*, 29.
(65) McClain, W. M.; Harris, R. A. Two-photon molecular spectroscopy in liquids and gases. In *Excited States*; Lim, E. C., Ed.; Academic: New York, 1977; Vol. 3, p 1.
(66) Birge, R. R.; Pierce, B. M. *J. Chem. Phys.* **1979**, *70*, 165.
(67) Birge, R. R. *Acc. Chem. Res.* **1986**, *19*, 138.
(68) He, G. S.; Swiatkiewicz, J.; Jiang, Y.; Prasad, P. N.; Reinhardt, B. A.; Tan, L.-S.; Kannan, R. *J. Phys. Chem. A* **2000**, *104*, 4805.
(69) Kannan, R.; He, G. S.; Yuan, L.; Xu, F.; Prasad, P. N.; Dombroskie, A. G.; Reinhardt, B. A.; Baur, J. W.; Vaia, R. A.; Tan, L.-S. *Chem. Mater.* **2001**, *13*, 1896.
(70) Rijkenberg, R. A.; Bebelaar, D.; Buma, W. J.; Hofstraat, J. W. *J. Phys. Chem. A* **2002**, *106*, 2446.
(71) Bayliss, N. S.; McRae, E. G. *J. Phys. Chem.* **1954**, *58*, 1002.
(72) McRae, E. G. *J. Phys. Chem.* **1957**, *61*, 562.
(73) McRae, E. G. *Spectrochim. Acta* **1958**, *12*, 192.
(74) Cooper, T. M.; Natarajan, L. V.; Soward, L. A.; Spangler, C. W. *Chem. Phys. Lett.* **1999**, *310*, 508.
(75) Onsager, L. *J. Am. Chem. Soc.* **1936**, *58*, 1486.
(76) Karelson, M.; Tamm, T.; Zerner, M. C. *J. Phys. Chem.* **1993**, *97*, 11901.
(77) Schulte-Frohlinde, D.; Blume, H.; Gusten, H. *J. Phys. Chem.* **1962**, *66*, 2486.
(78) Reichardt, C. *Solvents and Solvent Effects in Organic Chemistry*, 2nd ed.; VCH Publishers: New York, 1988.

(79) Rogers, J. E.; Fleitz, P. A. To be published, 2004.
(80) Baumann, W.; Deckers, H.; Loosen, K.-D.; PetzKe, F. *Ber. Bunsen-Ges. Phys. Chem.* **1977**, *81*, 799.
(81) Liptay, W. Dipole Moments and Polarizabilities of Molecules in Excited Electronic States. In *Excited States*; Lim, E. C., Ed.; Academic Press: New York, 1974; Vol. 1, p 129.
(82) Swalen, J. D.; Moylan, C. R. Linear Optical Properties. In *Characterization Techniques and Tabulations for Organic Nonlinear Optical Materials*; Kuzyk, M. G., Dirk, C. W., Eds.; Marcel Dekker AG: New York, 1998; p 223.
(83) Delysse, S.; Raimond, P.; Nunzi, J.-M. *Chem. Phys.* **1997**, *219*, 341.
(84) Bree, A.; Zwarich, R. *J. Chem. Phys.* **1969**, *51*, 903.
(85) Berlman, I. B. *J. Chem. Phys.* **1970**, *52*, 5616.
(86) Drucker, R. P.; McClain, W. M. *J. Chem. Phys.* **1974**, *61*, 2616.
(87) Rumi, M.; Perry, J. W. Investigation of Air Force two-photon dyes. University of Arizona, 2002.
(88) Negres, R. A.; Hales, J. M.; Kobyakov, A.; Hagan, D. J.; Stryland, E. W. V. *IEEE J. Quantum Electron.* **2002**, *38*, 1205.
(89) Belfield, K. D.; Schafer, K. J.; Mourad, W.; Reinhardt, B. A. *J. Org. Chem.* **2000**, *65*, 4475.
(90) Schafer, K. J.; Hales, J. M.; Balu, M.; Belfield, K. D.; Van Stryland, E. W.; Hagan, D. J. *J. Photochem. Photobiol., A* **2004**, *162*, 497.
(91) Belfield, K. D.; Hagan, D. J.; Van Stryland, E. W.; Schafer, K. J.; Negres, R. A. *Org. Lett.* **1999**, *1*, 1575.
(92) Okawara, M.; Kitao, T.; Hirashima, T.; Matsuoka, M. *Organic Colorants, a handbook of data of selected dyes for electro-optical applications*; Kodansha Ltd. and Elsevier Science Publishers B. V.: Tokyo and Amsterdam, 1988.
(93) Czekalla, J.; Wick, G. *Ber. Bunsen-Ges. Phys. Chem.* **1961**, *65*, 727.
(94) Cheng, L.-T.; Tam, W.; Marder, S. R.; Stiegman, A. E.; Rikken, G.; Spangler, C. W. *J. Phys. Chem.* **1991**, *95*, 10643.
(95) *Spectral Atlas of Polycyclic Aromatic Compounds*; Karcher, W., Devillers, J., Garrigues, P., Jacob, J., Eds.; D. Reidel Pub. Co.: Boston, MA, 1988; Vol. 2.
(96) Mukherjee, N.; Mukherjee, A.; Reinhardt, B. A. *Appl. Phys. Lett.* **1997**, *70*, 1524.
(97) He, G. S.; Lin, T.-C.; Dai, J.; Prasad, P. N.; Kannan, R.; Dombroskie, a. A. G.; Vaia, R. A.; Tan, L.-S. *J. Chem. Phys.* **2004**, *120*, 5275.
(98) Swiatkiewicz, J.; Prasad, P. N.; Reinhardt, B. A. *Opt. Commun.* **1998**, *157*, 135.
(99) Kim, O.-K.; Lee, K.-S.; Woo, H. Y.; Kim, K.-S.; He, G. S.; Swiatkiewicz, J.; Prasad, P. *Chem. Mater* **2000**, *12*, 284.
(100) Nafiatis, F.; Rogers, J. Unpublished material, 2003.
(101) Belfield, K. D.; Bondar, M. V.; Przhonska, O. V.; Schafer, K. J.; Mourad, W. *J. Lumin.* **2002**, *97*, 141.
(102) Drenser, K. A.; Larsen, R. J.; Strohkendl, F. P.; Dalton, L. R. *J. Phys. Chem. A* **1999**, *103*, 2290.
(103) Fleitz, P. A.; Brandt, M. C.; Sutherland, R. L.; Strohkendl, F. P.; Larsen, R. J.; Dalton, L. R. TPA exp for af50. SPIE conference on Nonlinear Optical Liquids for Power Limiting and Imaging, 1998.
(104) Chung, M.-A.; Lee, K.-S.; Jung, S.-D. *ETRI J.* **2002**, *24*, 221.